

Worked in different universities/institutions in various capacities as follows:

From the Selected Works of Dr. Mohammad Mansoob Khan

May 28, 2013

Simultaneous enhancement of the methylene blue degradation and power generation in microbial fuel cell by gold nanoparticles

Mohammad Mansoob Khan, Dr

T. H. Han

S. Kalathil

J. Lee

M. H. Cho



SELECTEDWORKS™

Available at: http://works.bepress.com/mmansoob_khan/29/

Simultaneous Enhancement of Methylene Blue Degradation and Power Generation in a Microbial Fuel Cell by Gold Nanoparticles

Thi Hiep Han, Mohammad Mansoob Khan, Shafeer Kalathil, Jintae Lee, and Moo Hwan Cho*

School of Chemical Engineering, Yeungnam University, Gyeongsan, Gyeongbukdo 712-749, South Korea

Supporting Information

ABSTRACT: This study examined the effect of positively charged gold nanoparticles [(+)AuNPs] on the enhancement of methylene blue (MB) degradation in a microbial fuel cell (MFC) cathode. Complete MB degradation and a maximum electricity production of 36.56 mW/m² were achieved simultaneously. The MFC performance and MB degradation were found to be strictly dependent on the cathodic conditions, such as N₂ bubbling, air bubbling, and addition of H₂O₂. MB was reduced rapidly under anaerobic conditions, whereas complete oxidative mineralization of MB occurred in the presence of dissolved oxygen (DO) or H₂O₂. (+)AuNPs enhanced the electricity generation in the MFCs involving MB degradation owing to its electron-relay effect. The presence of both (+)AuNPs and H₂O₂ produced the greatest enhancement in MB degradation. After 5 h, almost all of the MB (98%) and chemical oxygen demand (COD) (96%) had been removed in the presence of (+)AuNPs, whereas only 57.4% of the MB and 40% of the COD had been removed in the absence of (+)AuNPs.

1. INTRODUCTION

Methylene blue (MB) is a heterocyclic aromatic dye that is extensively used for dyeing cotton, wool, and silk.¹ The presence of this dye in wastewater can cause a severe threat to humans (nausea, vomiting, and diarrhea)¹ and the environment because of its intense color and toxicities.² A number of methods have been used for the treatment of such dye-containing wastewaters, including physical methods employing precipitation, adsorption, and reverse osmosis; chemical methods such as oxidation (using air, oxygen, ozone, NaOCl, and H₂O₂ as oxidants) and reduction (Na₂S₂O₄); and biological methods such as aerobic and anaerobic treatments.³ Each of these treatments has special advantages, but intense energy input, sludge formation, and the development of toxic intermediates are common challenges⁴ that need to be solved before these approaches can be used more widely.

Recently, the simultaneous degradation of dye wastewater and generation of electricity using microbial fuel cells (MFCs) has attracted considerable attention as an economical and environmentally friendly technique.^{5,6} MFCs are bioelectrochemical devices that use bacteria as catalysts to produce electricity by oxidizing organic and inorganic compounds in biomass.⁷ A typical MFC contains an anaerobic anode chamber and an aerobic cathode chamber separated by a proton-exchange membrane. An external circuit connects the anode and cathode.⁸ Theoretically, any compound with sufficiently high redox potentials can serve as a cathodic electron acceptor in an MFC.⁹ Thus far, dyes can be used as an alternative cathodic electron acceptor in place of air in MFCs.^{10–12} AuNPs have attracted considerable attention for applications in medicine, biotechnology, nanoscale electronics, and catalysis and are the most intensively studied nanoparticles.^{13–15} Catalysis is one of the fastest growing lines of AuNP research.¹⁶ AuNPs are effective catalysts for the degradation of MB and other dyes.^{17–20} The catalytic activity of AuNPs can be considerably affected by particle size and shape,²¹ as well as

charge state.²² In dye degradation catalyzed by AuNPs, the catalytic activity of AuNPs is significantly affected by the dye characteristics, such as the adsorption of the dye on the AuNPs and the hydrophobicity of the dye.¹⁷ To the best of our knowledge, there are no reports of the use of positively charged gold nanoparticles [(+)AuNPs] in the cathode of an MFC as a catalyst for MB degradation. This study examined the feasibility of the direct utilization of a heterocyclic aromatic dye as an electron acceptor in the presence of (+)AuNPs in the MFC cathode. In addition, the power generation of the MFC and the MB degradation rate in the presence and absence of (+)AuNPs were determined. Moreover, the effects of different cathode conditions, such as N₂ bubbling (anaerobic), air bubbling (aerobic), addition of H₂O₂, pH, and different types of AuNPs (positive and negative charge), on the MB degradation rate and power output of MFCs were examined.

2. MATERIALS AND METHODS

2.1. Materials. MB was obtained from Junsei Chemical Co. (Seoul, South Korea) and used as received. Hydrogen tetrachloroaurate(III) hydrate (HAuCl₄·nH₂O, *n* = 3.6) was purchased from Kojima Chemical Co. (Saitama, Japan). The other basic chemicals, such as hydrogen peroxide (H₂O₂), sodium hydroxide (NaOH), sodium acetate (CH₃COONa), phosphoric acid (H₃PO₄), sodium phosphate monobasic (NaH₂PO₄), and sodium phosphate dibasic (NaH₂PO₄), were supplied by Duksan Pure Chemical Co. (Ansan, South Korea). Carbon paper (without wet-proofing) and Pt-coated carbon paper (0.5 mg of Pt/cm²) were purchased from Fuel Cell Earth LLC Co. (Stoneham, MA). Deionized distilled water was used in all experiments.

Received: February 28, 2013

Revised: April 30, 2013

Accepted: May 27, 2013

Published: May 27, 2013

2.2. Synthesis of AuNPs. The (+)AuNPs were synthesized using a stainless steel mesh, as reported earlier.²³ Briefly, a 1 mM HAuCl₄ aqueous solution (100 mL) was prepared and adjusted to pH 4 using 0.1 M NaOH. A piece of stainless steel mesh (2.5 cm × 4.5 cm) was dipped in the resulting solution. The reaction mixture was kept stirring at room temperature. The initial pale yellow color of the precursor changed to a ruby red color within 1 h, indicating the formation of (+)AuNPs. The as-synthesized (+)AuNPs were positively charged (+24.2 mV) and 5–20 nm in size. Figure S1 (Supporting Information) presents a transmission electron microscopy (TEM) image and an X-ray diffraction (XRD) pattern of the as-synthesized (+)AuNPs.

Citrate-capped AuNPs were synthesized using the Turkevich method.²⁴ The citrate-capped AuNPs had a negative charge and a mean diameter of 17 nm.

2.3. MFC Construction and Operation. To examine the catalytic activity of the (+)AuNPs in MB degradation in an MFC cathode, two of the same MFC systems, in the presence and absence (control MFC) of (+)AuNPs were operated simultaneously. The MFCs were constructed as described previously.²⁵ The MFCs consisted of two identical chambers (anode and cathode chambers) separated by a Nafion membrane. Each chamber had an effective volume of 250 mL (Corning Inc.; 300 mL capacity). The bottles were joined by two clamps between the flattened ends of the two glass tubes (inner diameter = 1.3 cm) fitted with rubber gaskets. In the anode chamber, an electrochemically active biofilm (EAB) was developed on plain carbon paper (2.5 cm × 4.5 cm) in artificial wastewater using sodium acetate as the electron donor (1 g/L). A mineral salt medium²⁵ was added to the anode chamber and inoculated with 10 mL of anaerobic sludge (from a biogas plant in Paju, South Korea). The anode chamber was bubbled with nitrogen for 10 min to remove any oxygen (anode pH ≈ 7.4).

Initially, conventional H-type MFCs were operated to obtain efficient MFC systems for the experiments²⁵ using Pt-coated carbon paper as the cathode electrode. The cathode chamber was filled with a phosphate buffer solution (PBS, 50 mM) and bubbled continuously with air. After 1 week of continuous operation, the MFCs produced a stable power density of 40 mW/m² (data not shown), which matched previous results.²⁶ After stable power had been obtained, the catholyte was replaced with 200 mL of 50 mM PBS containing 16 mg/L MB and 50 mL of the as-synthesized (+)AuNP colloidal solution, where the latter was sonicated for 5 min before being added to the MFC cathode. The final concentration of (+)AuNPs used at the cathode was 6.4 nM. The Pt-coated carbon paper was then replaced with plain carbon paper. In all the experiments, the MFCs were connected to a resistance box at 1000 Ω, and the process was conducted at 30 °C under atmospheric pressure. For comparison, a control MFC was operated simultaneously without addition of (+)AuNPs. A magnetic stirrer was used continuously to agitate the MFC catholyte.

2.4. Cyclic Voltammetry (CV). CV measurements were carried out on a potentiostat (VersaSTAT 3, Princeton Applied Research, Oak Ridge, TN) using a standard three-electrode system. Ag/AgCl (saturated with KCl, Ag/AgCl, +0.197 V) was used as the reference electrode. A Pt wire gauge was used as the counter electrode. Carbon paper was used as the working electrode. MB in 50 mM PBS (pH 3) in the presence and absence of (+)AuNPs at the same concentrations as used in the MFC catholyte was used for cyclic voltammetry.

2.5. Calculation and Analysis. The voltage was recorded every 2 min using a digital multimeter (Agilent 34405A, Palo Alto, CA). The power (*P*) was calculated using the equation $P = IV$, where *I* is the current and *V* is the voltage, which were normalized to the surface area of the anode electrode.

The MB degradation was evaluated from the decrease in the absorbance of MB using a UV–vis spectrophotometer (Optizen 2120 UV, Mecasys Co., Daejeon, South Korea). The degradation efficiency of MB was calculated using the equation degradation (%) = $[(C_0 - C_t)/C_0] \times 100\%$, where *C*₀ and *C*_{*t*} are the original and residual concentrations, respectively, of MB in the catholyte.

To assess the impact of pH on the MB degradation, the pH of PBS was varied from 3 to 7 by adjusting the composition of H₃PO₄, NaH₂PO₄, and NaH₂PO₄.¹¹ The pH was measured using a digital pH meter (HANNA Instruments, Smithfield, RI).

To assess the impact of the dissolved oxygen (DO) concentration on the MFC performance and MB degradation, air at different flow rates of 0, 30, and 60 mL/min was bubbled in the MFC cathode. The DO concentration was measured using a DO meter (HI 91410, HANNA Instruments, Smithfield, RI).

The chemical oxygen demand (COD) was measured using the Reactor Digestion method with a Hach DR/2500 spectrophotometer (Hach, Loveland, CO).

3. RESULTS AND DISCUSSION

3.1. MFC Performance and MB Reduction under Anaerobic Conditions. Two MFC systems in the presence and absence of 50 mL of the as-synthesized (+)AuNP colloidal solution in the cathode were operated in parallel. The cathode was bubbled continuously with pure N₂. Under these conditions, (+)AuNPs enhanced the maximum power density by approximately 1.7-fold. Maximum power densities of 35.6 and 20.6 mW/m² were observed in the presence and absence, respectively, of the (+)AuNPs with an external resistance of 1000 Ω (Figure 1a). In the presence of (+)AuNPs, the power generation remained stable for 2 h and then decreased sharply because of a decrease in the MB concentration in the MFC cathode. In the absence of (+)AuNPs, power generation decreased significantly in the first 2 h. In both cases, power generation was almost negligible after 4 h, indicating the complete disappearance of MB. When fresh MB was added, the power generation was regained in both systems. These results suggest that the MFC system can be used to generate electricity continuously by replacing the MB.¹¹

The reduction of MB in the MFC cathode correlated with the power generation. The UV–vis absorption spectra in Figure 2 show that the MB peaks decreased gradually and almost disappeared, corresponding to the disappearance of the blue color after 4 h. Concomitantly, an absorption peak at 256 nm gradually appeared, which confirmed the formation of leuco-methylene blue (LMB).²⁷ This suggests that the MB in the MFC cathode was reduced completely to LMB after 4 h, because the (+)AuNPs behave as an electron-relay catalyst, which facilitates the reduction of MB to LMB.²⁸ As a result, faster MB reduction and higher power generation were achieved.

3.2. MFC Performance and MB Oxidation under Aerobic Conditions. Two MFCs were run simultaneously with the continuous bubbling of air at the cathode at different flow rates of 0, 30, and 60 mL/min. Under these conditions, the

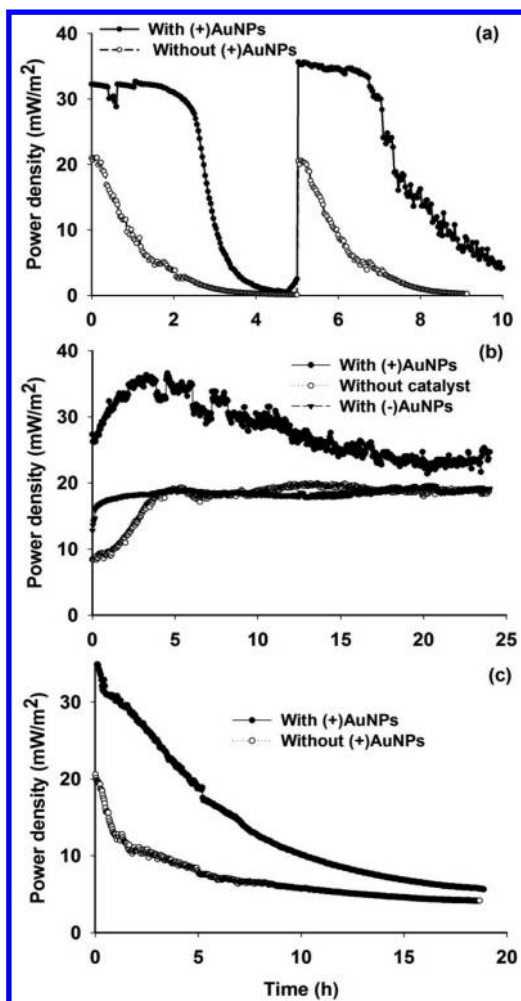


Figure 1. Power density profile of MFCs in the presence and absence of (+)AuNPs (a) under anaerobic conditions, (b) under aerobic conditions with air bubbling at 30 mL/min, and (c) upon addition of 0.176 mM H₂O₂. Experimental conditions: 16 mg/L MB, 50 mL (+)AuNPs, pH 3.

(+)AuNPs enhanced the power generation of the MFC approximately 2-fold. A maximum power generation of 36.56 and 19.05 mW/m² was obtained in the presence and absence of (+)AuNPs, respectively. The performance of the cathodic MFC under aerobic conditions was completely different from that under anaerobic conditions. Figure 1b shows that, during aeration, the power generation always maintained a high value, even after MB had been degraded completely. This power was maintained by O₂, which is a well-known cathodic electron acceptor in MFC cathodes.²⁹

Figure 3 shows typical temporal spectral changes in MB under aerobic conditions (at an air bubbling rate of 30 mL/min). The MB peaks decreased gradually with time in both MFC systems. After 24 h, the MB peak almost disappeared (91.8%) in the presence of (+)AuNPs, whereas only 68.2% of the MB was degraded in the absence of (+)AuNPs. In contrast to the anaerobic cathodic MFCs, no new peak for intermediates appeared during MB degradation (Figure 3). The bands at 246 and 292 nm, which were originally present in the MB spectra, first increased and then decreased significantly with increasing reaction time. This means that complete oxidative decomposition of the phenothiazine species occurred and that other intermediates containing the phenothiazine moiety no longer

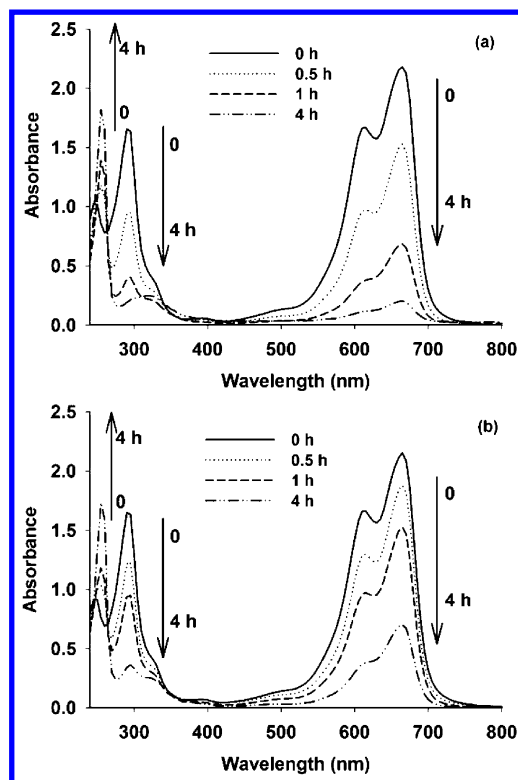


Figure 2. Absorption spectral changes of MB aqueous solution in the MFC cathode in the (a) presence and (b) absence of (+)AuNPs under anaerobic conditions. Experimental conditions: 16 mg/L MB, 50 mL (+)AuNPs, pH 3.

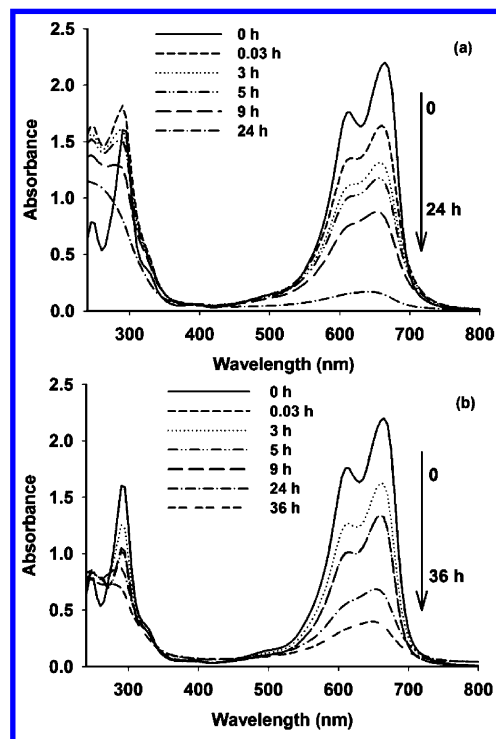


Figure 3. Absorption spectral changes of MB aqueous solution in the MFC cathode in the (a) presence and (b) absence of (+)AuNPs under aerobic conditions. Experimental conditions: 16 mg/L MB, 50 mL (+)AuNPs, pH 3, air bubbling flow rate of 30 mL/min.

existed.³⁰ More concrete evidence for the mineralization of MB is provided by the fact that almost no COD remained after MB degradation (Table 1).

Table 1. COD Values before and after Reaction under Different Cathode Conditions

experimental conditions	reaction time (h)	COD (mg/L)	
		with (+) AuNPs	without (+) AuNPs
N ₂ bubbling, pH 3	0	37 ± 2.5	38 ± 3.5
	5	34 ± 1	35 ± 0.5
air bubbling, 30 mL/min, pH 3	0	38 ± 4	37 ± 3
	24	9 ± 1	29 ± 2
0.176 mM H ₂ O ₂ , pH 3	0	38 ± 3	35 ± 2.5
	5	1.5 ± 0.1	21 ± 2

Another observation in the UV-vis spectra of MB is the initial decrease in the peak intensity at 660 nm (Figure 3a). This is probably due to the adsorption of MB on the surfaces of the (+)AuNPs and carbon electrode. From the decrease in the initial peak intensity, the percentage adsorption of MB on the (+)AuNPs and carbon paper was approximately 15%, which suggests that only approximately 85% of the MB contributed to power generation in the MFCs.

The effects of different DO concentrations on MB degradation were examined by changing the air bubbling rate to 0, 30, and 60 mL/min, corresponding to average DO concentrations of 7.8 ± 0.1 , 8.2 ± 0.1 , and 8.5 ± 0.2 mg/L (saturated DO), respectively (experimentally measured). The DO values varied because DO was consumed during the reaction. Here, the DO values were measured in triplicate in the cathode, and the average was taken after 0, 9, and 24 h of reaction. Figure 4a shows that the MB degradation rate increased when the air bubbling rate was increased from 0 to 30 mL/min. A further increase in the air bubbling rate to 60 mL/min did not increase the MB degradation rate. This suggests that an air bubbling rate of 60 mL/min (corresponding to a DO level of 8.2 mg/L) meets the requirements for MB degradation.

3.3. Enhancement of MB Oxidation by Addition of H₂O₂ in the Cathode. Adding H₂O₂ to the reaction mixture is an effective method for enhancing the dye degradation rate through the formation of hydroxyl (\cdot OH) radicals.³¹ Thus, in this study, H₂O₂ was added to the cathode chamber with no air or N₂ bubbling to enhance the MB oxidation rate. This condition can be considered as the addition of H₂O₂ under aerobic condition with no air bubbling. In the case of no addition of H₂O₂, the time required for complete MB degradation was 48 h, whereas upon the addition of 0.176 mM H₂O₂, complete MB degradation was obtained in 19 h.

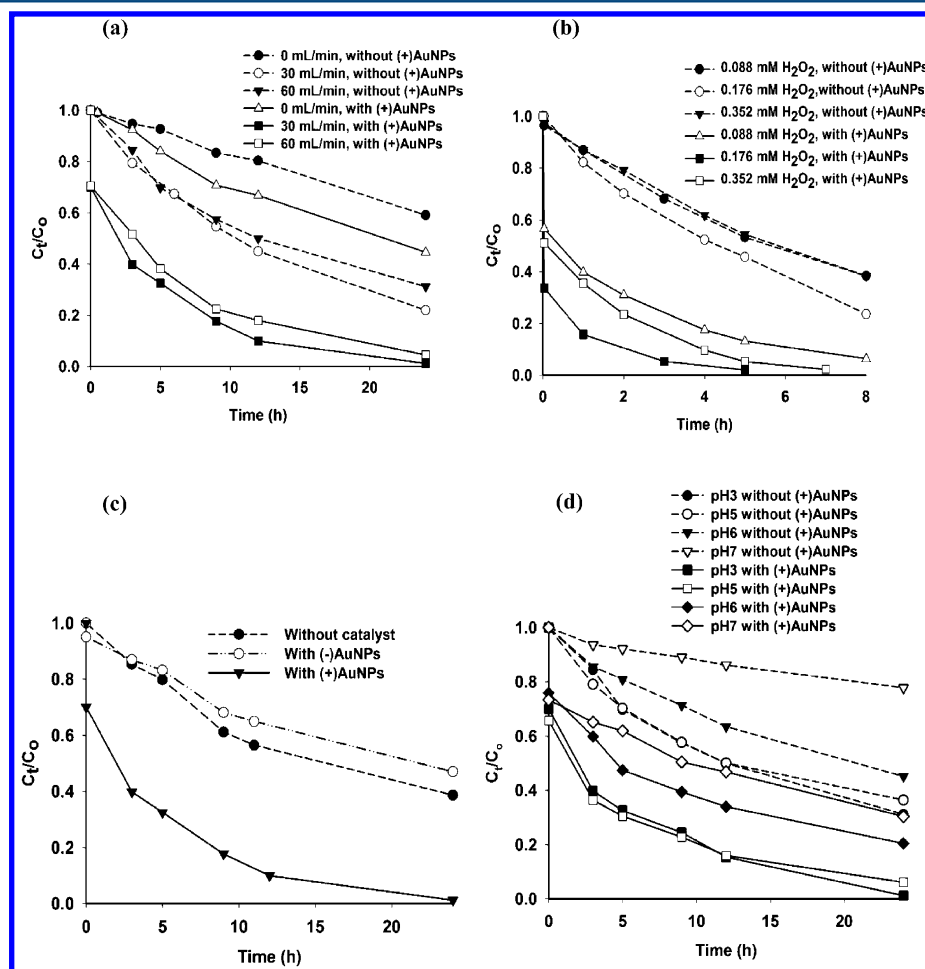


Figure 4. Dependence of the degradation kinetics of MB in the presence and absence of (+)AuNPs on the (a) air bubbling rate, (b) H₂O₂ concentration, (c) catalyst charge, and (d) catholyte pH. Aside from the investigated parameter, the other parameters were fixed as follows: 16 mg/L MB, 50 mL catalyst, pH 3, air bubbling rate of 30 mL/min.

The time for MB degradation was significantly shortened in the presence of both (+)AuNPs and 0.176 mM H_2O_2 , which required 2 h for almost-complete MB degradation. These results indicate that a great enhancement in MB degradation was obtained in the presence of both (+)AuNPs and H_2O_2 .

Figure 5 shows typical temporal spectral changes in MB after addition of 0.176 mM H_2O_2 . Immediately after the addition of

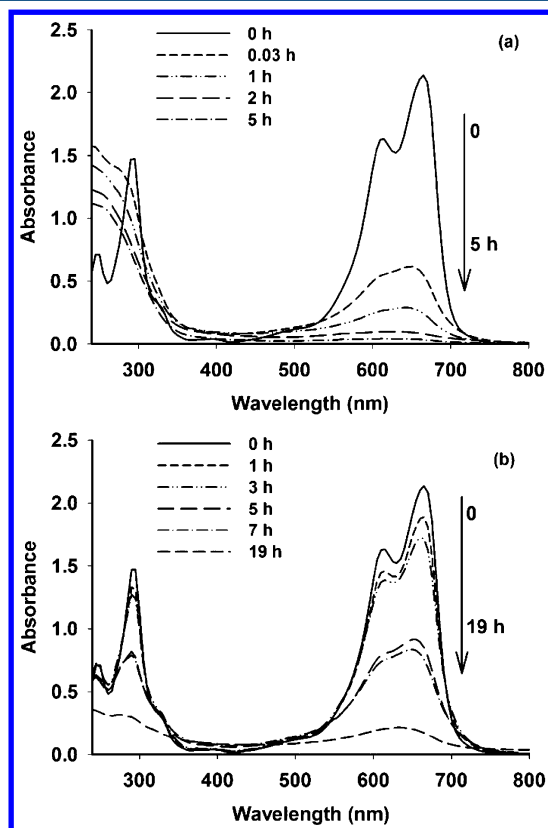
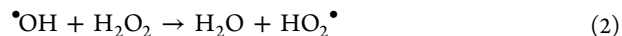


Figure 5. Absorption spectral changes of MB aqueous solution in the MFC cathode with initial addition of 0.176 mM H_2O_2 in the (a) presence and (b) absence of (+)AuNPs. Experimental conditions: 16 mg/L MB, 50 mL (+)AuNPs, pH 3.

H_2O_2 , a dramatic decrease in the UV–vis peak was observed, which corresponds to more than 60% MB degradation. Almost all of the MB (97.4%) had degraded after 5 h in the presence of (+)AuNPs, whereas only 57% of the MB had degraded in the absence of (+)AuNPs. The faster MB degradation in the presence of (+)AuNPs could be due to the larger amount of $\cdot\text{OH}$ radicals that formed on the (+)AuNP surface.³²

Moreover, it was found that the MB degradation was H_2O_2 -dose-dependent. After addition of H_2O_2 at concentrations of 0.088, 0.176, and 0.352 mM, the rate of MB degradation first increased and then decreased (Figure 4b). With the addition of 0.088 mM H_2O_2 , the MB degradation efficiency was 86.9% [with (+)AuNPs] and 46.8% [without (+)AuNPs], and it reached 97.4% [with (+)AuNPs] and 54.3% [without (+)AuNPs] at a H_2O_2 concentration of 0.176 mM. When the amount of H_2O_2 was increased further to 0.352 mM, the MB degradation efficiency decreased to 94.7% [with (+)AuNPs] and 45.6% [without (+)AuNPs]. The initial increase in the MB degradation efficiency can be attributed to the formation of more $\cdot\text{OH}$ radicals, which are responsible for MB degradation (eq 1).³¹ On the other hand, at higher concentrations, the

H_2O_2 could effectively scavenge $\cdot\text{OH}$ radicals to produce $\text{HO}_2\cdot$ radicals (eq 2). Because $\text{HO}_2\cdot$ is less reactive than $\cdot\text{OH}$, it makes a negligible contribution to MB degradation.³¹ Therefore, the optimal H_2O_2 concentration for MB degradation in this study was found to be 0.176 mM.



The MFC power generation profile correlated well with the MB degradation. The initial highest power generation observed was 35.5 and 20.56 mW/m^2 in the presence and absence, respectively, of (+)AuNPs. As MB degraded quickly in the first 5 h, the power generation also decreased dramatically during this time. Once MB had been completely oxidized, the power generation was maintained at 9 and 7 mW/m^2 in the presence and absence, respectively, of (+)AuNPs (Figure 1c).

3.4. Effect of the Charge and pH of AuNPs on MB Degradation. A control experiment with negatively charged gold nanoparticles [(−)AuNPs] was performed to examine the effect of the charge of the catalyst on MB degradation in an MFC cathode. As expected, the MFC power generation (Figure 1b) and MB degradation rate (Figure 4c) in the presence of (−)AuNPs were similar to those of the control system and much lower than those of (+)AuNPs. In contrast to (+)AuNPs, (−)AuNPs repel electrons. This repulsion inhibits electron relay and decreases the electron-transfer rate. Consequently, (−)AuNPs cannot capture and relay the electrons and, thus, catalyze MB degradation in the MFC cathode, leading to a decline in the MB degradation rate and power generation. These results suggest that the charge of the AuNP catalyst plays a key role in catalyzing MB degradation in the MFC cathode.

Because the involvement of protons in the degradation¹¹ and pH can affect the positive charge of AuNPs,²³ it is very important to control the pH in the MFC cathode, especially when real dye wastewater with a wide range of pH values is used. Comparative experiments were performed at four different pH values (3, 5, 6, and 7) with the other parameters kept constant. Figure 4d presents the results for the MB degradation rate at different pH values. At low pH (pH 3), the MB degradation efficiency reached 98.8% [with (+)AuNPs] and 83.3% [without (+)AuNPs]. When the pH of the MB solution was increased from 3 to 5, the MB degradation efficiency decreased to 93.9% [with (+)AuNPs] and 68.8% [without (+)AuNPs]. Finally, the MB degradation efficiency decreased to 79.5% [with (+)AuNPs] and 43% [without (+)AuNPs] at pH 6 and to 69.6% [with (+)AuNPs] and 22.2% [without (+)AuNPs] at pH 7. These results show that MB degradation occurred more easily at low pH rather than at high pH, in agreement with a previous study.¹¹

The effect of pH on the system can be explained in terms of the relationship between the pH and the charge of (+)AuNPs. The as-synthesized (+)AuNP colloidal solution is highly positive charged at pH 3. An increase in pH causes the loss of positive charge, as reported in our previous study.²³ More significantly, an increase in pH causes a decline in the redox potential and, thus, the cell voltage.¹¹ Therefore, the loss of positive charge on the (+)AuNPs due to the increase in pH of the (+)AuNPs also causes a decrease of the redox potential, corresponding to the decline of the reaction rate and power generation. This claim was confirmed by the decline in MFC power generation (Figure 1b) and MB degradation rate (Figure 4c) when the (+)AuNPs were replaced by (−)AuNPs.

3.5. MB Degradation Based on COD Removal. The COD values of the MB solution before and after the reaction were measured to determine whether the MB was actually mineralized at the MFC cathode. Table 1 lists the COD values before and after the reaction under different MFC cathode conditions. The COD removal efficiency was quite high in the case of air or H_2O_2 supplied to the cathode. For air, COD reductions of approximately 76% and 22% were achieved after 24 h in the presence and absence, respectively, of (+)AuNPs. After the addition of H_2O_2 , the COD removal efficiencies after 5 h were 96% and 40% in the presence and absence, respectively, of (+)AuNPs (Table 1). On the other hand, for MB reduction under anaerobic conditions (N_2 bubbling), only a small quantity of COD (approximately 8%) was removed. Even after the bubbling of N_2 , not all of the DO was removed and approximately 0.6 mg/L remained, which was responsible for the low percentage of MB oxidation and ultimately the small decrease in COD.³⁰ A combination of the UV-vis spectral data with the COD data shows that oxidative mineralization did not occur under anaerobic conditions and occurred only in the presence of oxygen or H_2O_2 .

3.6. Mechanism of Enhanced Performance of MFC and MB Degradation by (+)AuNPs. The electrochemical behavior of the (+)AuNPs toward MB degradation in the MFC cathode was examined by CV. As shown in Figure 6, CV

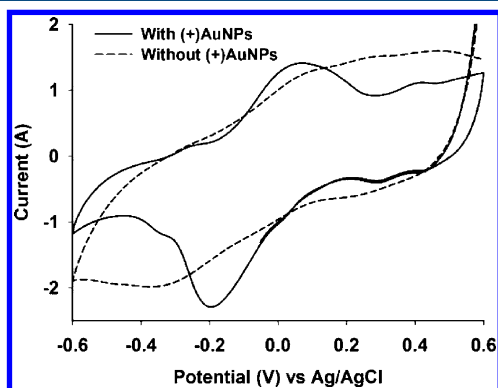
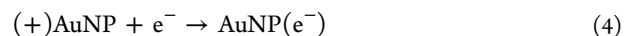


Figure 6. Cyclic voltammograms for 0.05 mM MB in the presence and absence of 50 mM (+)AuNPs in 50 mM PBS at pH 3. Scan rate = 0.5 V/s.

revealed well-defined oxidation and reduction peaks induced by the (+)AuNPs. This suggests that the electrochemical activity of the MFC cathode was promoted by (+)AuNPs, which supports the enhancement of electricity generation by (+)AuNPs.

The mechanism of enhancement of MB degradation in an MFC cathode by (+)AuNP catalyst is described in Figure 7. In the anode chamber of an MFC, the EAB on carbon paper oxidizes acetate to produce electrons and protons. The protons then permeate to the cathode chamber through the Nafion membrane, whereas the electrons are transferred from the anode to the cathode through an external circuit. In the absence of a catalyst, the dye itself can act as an electron acceptor in the MFC cathode.¹¹ Thus, MB can capture electrons and protons directly for the reduction of MB to LMB (eq 3). In the presence of (+)AuNP catalyst, which are well-known as a powerful electron capturer,^{16,33} (+)AuNPs catch the coming electrons immediately to yield $\text{AuNP}(\text{e}^-)$ (eq 4). The MB molecules then capture electrons from (+)AuNPs and are reduced to the LMB (eq 5). The formation of LMB is confirmed by the appearance of an absorption peak at 256 nm in absorption spectra (Figure 2). The LMB peak then increases continuously with time until MB reduction is finished without the appearance of other intermediate peaks. This indicates that, under anaerobic conditions (without oxygen or H_2O_2), the reduction of MB to LMB occurs, with LMB being the final product. In this case, (+)AuNPs relay the electrons from the cathode to MB and enhance the reaction rate.



In addition to these reactions, under aerobic conditions, DO can accept electrons stored in the $\text{AuNP}(\text{e}^-)$ to form superoxide (O_2^\bullet) radicals (eq 6), which can destroy the toxic intermediates.³⁴ Thus, LMB can be readily mineralized to other products by free radicals (eq 7), as confirmed by the absence of an LMB peak in the absorption spectra (Figures 3 and 5). In fact, the direct mineralization of MB can occur simultaneously with LMB (eq 7).³⁵

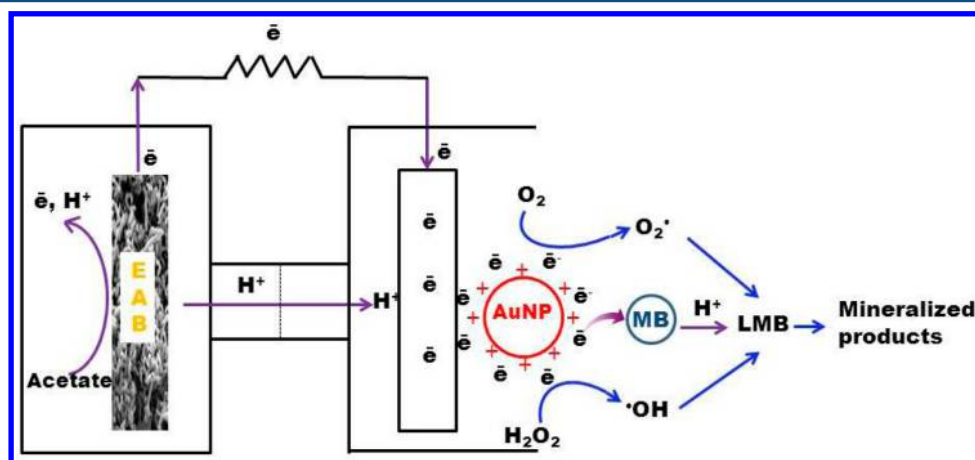
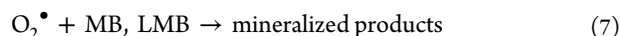
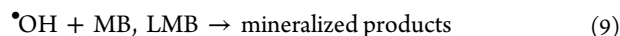


Figure 7. Schematic diagram of the proposed mechanism of MB degradation in the MFC cathode.



Similarly to oxygen, H_2O_2 can also receive electrons to produce $\bullet\text{OH}$ as the main free radical (eq 8).³¹ Thus, for the addition of H_2O_2 in the MFC cathode, in addition to O_2^\bullet radicals being formed by DO, a large amount of $\bullet\text{OH}$ radicals are also formed, which helps to enhance the degradation of MB (eq 9).



In these cases, (+)AuNPs relay electrons from the cathode to electron acceptors, such as oxygen and H_2O_2 . The relay effect of (+)AuNPs might increase the generation of O_2^\bullet or $\bullet\text{OH}$ radicals, which would enhance the oxidation reaction rate. The electron-relay activity of (+)AuNPs for dye reduction has been well-established.^{19,20,36}

An interesting phenomenon was observed that after treatment under anaerobic conditions, the blue color of MB was restored when the treated solution was removed from the MFC cathode and exposed to atmospheric oxygen. A likely reason for this behavior is that LMB can be readily oxidized to the MB precursor by atmospheric oxygen. The same phenomenon has also been reported elsewhere.³⁰ On the contrary, after treatment under aerobic conditions, no restoration of MB was observed. This suggests that no LMB remained in suspension after treatment under aerobic conditions. This observation matches our proposed mechanism that, under aerobic conditions, MB was completely oxidized to other mineral products. The complete oxidation of MB can be confirmed by (i) the lack of restoration of MB after treatment, (ii) the lack of COD remaining in treated suspension, and (iii) the lack of an intermediate peak in the UV spectrum.

The MB reduction under anaerobic conditions was fast, but the power generation was low and interrupted. Another disadvantage was that intermediate product still remained in the effluent. Even though MB oxidation under aerobic conditions takes a longer time, complete MB oxidation as well as high and stable power generation can be achieved. Moreover, the reaction time of MB oxidation under aerobic conditions can be shortened to several hours by the initial addition of a small amount of H_2O_2 (0.176 mM). Thus, it is suggested that MB oxidation in an MFC cathode under aerobic conditions is a better method for practical application. Compared to other physical or chemical methods for MB degradation, MB oxidation in an MFC cathode under aerobic conditions requires low energy input (note that MB oxidation can also occur with no air bubbling and no chemical input), high efficiency (almost all of the MB was removed), and no production of toxic intermediates. In particular, in addition to complete MB degradation, a high power density was achieved using this process. Moreover, other types of MFCs or scale-up reactors can be applied to achieve higher power densities. Even though this process uses an expensive (+)AuNP catalyst, the catalyst can be recycled and used repeatedly without any significant change in catalytic activity (Figure S2a, Supporting Information). When the (+)AuNPs were reused, the MB degradation efficiency was 90.1% after 24 h, slightly less than the 98.77% value obtained for the use of fresh (+)AuNPs (Figure S2b, Supporting Information), and the maximum power generation was slightly reduced from 36.56 to 32 mW/ m^2 (data not shown). The method of recycling (+)AuNPs from

the cathode solution is presented in the Supporting Information. Therefore, this process is an effective and practical method for the degradation of MB. In addition to MB degradation, this process can be applied for other bioremediations.

4. CONCLUSIONS

(+)AuNPs can be used as a catalyst for simultaneous MB degradation and power generation in an MFC cathode. A maximum power generation of 36.56 mW/ m^2 and an MB degradation efficiency of 97.4% were achieved. (+)AuNPs played a role as an electron relay, thus enhancing MB degradation and power output by approximately 2-fold. In addition to power generation, the complete oxidative mineralization of MB can be accomplished without using external power. In particular, (+)AuNPs can be reused with stable MFC performance and MB degradation, which can reduce maintenance costs. Therefore, MB degradation in an MFC cathode has promising practical applications.

■ ASSOCIATED CONTENT

Supporting Information

TEM image, XRD pattern of as-synthesized (+)AuNPs. Method to collect and reuse (+)AuNPs. Kinetics and efficiency of MB degradation with fresh and reused (+)AuNPs. This material is available free of charge via the Internet at <http://pubs.acs.org>.

■ AUTHOR INFORMATION

Corresponding Author

*Tel.: 82-53-810-2517. Fax: 82-53-810-4631. E-mail: mhcho@ynu.ac.kr

Notes

The authors declare no competing financial interest.

■ ACKNOWLEDGMENTS

This study was supported by the Basic Science Research Program through the National Research Foundation of Korea (NRF) funded by the Ministry of Education, Science and Technology (2012R1A1A4A01005951).

■ REFERENCES

- (1) El-Sharkawy, E. A.; Soliman, A. Y.; Al-Amer, K. M. Comparative study for the removal of methylene blue via adsorption and photocatalytic degradation. *J. Colloid Interface Sci.* **2007**, *310*, 498.
- (2) Pant, D.; Singh, A.; Satyawali, Y.; Gupta, R. K. Effect of carbon and nitrogen source amendment on synthetic dyes decolorizing efficiency of white-rot fungus *Phanerochaete chrysosporium*. *J. Environ. Biol.* **2008**, *29*, 79.
- (3) Singh, K.; Arora, S. Removal of synthetic textile dyes from wastewaters: A critical review on present treatment technologies. *Crit. Rev. Environ. Sci. Technol.* **2011**, *41*, 807.
- (4) Armalar, P. F. F.; Fernandes, D. L. A.; Tavares, A. P. M.; Xavier, A. B. M. R.; Cammarota, M. C.; Coutinho, J. A. P.; Coelho, M. A. Z. Decolorization of dyes from textile wastewater by *trametes versicolor*. *Environ. Technol.* **2004**, *25*, 1313.
- (5) Kalathil, S.; Lee, J.; Cho, M. H. Granular activated carbon based microbial fuel cell for simultaneous decolorization of real dye wastewater and electricity generation. *New Biotechnol.* **2011**, *29*, 32.
- (6) Kalathil, S.; Lee, J.; Cho, M. H. Efficient decolorization of real dye wastewater and bioelectricity generation using a novel single chamber biocathode-microbial fuel cell. *Bioresour. Technol.* **2012**, *119*, 22.

- (7) Bond, D. R.; Holmes, D. E.; Tender, L. M.; Lovley, D. R. Electrode-reducing microorganisms that harvest energy from marine sediments. *Science* **2001**, *295*, 483.
- (8) Logan, B. E.; Hamelers, B.; Rozendal, R.; Schröder, U.; Keller, J. Microbial fuel cells: Methodology and technology. *Environ. Sci. Technol.* **2006**, *40*, 5181.
- (9) Li, Y.; Lu, A.; Ding, H.; Jin, S.; Yan, Y.; Wang, C.; Zen, C.; Wang, X. Cr(VI) reduction at rutile-catalyzed cathode in microbial fuel cells. *Electrochem. Commun.* **2009**, *11*, 1496.
- (10) Ding, H.; Li, Y.; Lu, A.; Jin, S.; Quan, C.; Wang, C.; Wang, X.; Zeng, C.; Yan, Y. Photocatalytically improved azo dye reduction in a microbial fuel cell with rutile-cathode. *Bioresour. Technol.* **2010**, *101*, 3500.
- (11) Liu, L.; Li, F.; Feng, C. Microbial fuel cell with an azo-dye-feeding cathode. *Appl. Microbiol. Biotechnol.* **2009**, *85*, 175.
- (12) Mu, Y.; Rabaey, K.; Rozendal, R. A.; Yuan, Z.; Keller, J. Decolorization of azo dye in bioelectrochemical systems. *Environ. Sci. Technol.* **2009**, *43*, 5137.
- (13) Haruta, M. Catalyst in the 21st century: Preparation, working mechanism and applications. *Gold Bull.* **2004**, *37*, 27.
- (14) Khan, M. M.; Lee, J.; Cho, M. H. Electrochemically active biofilm mediated bio-hydrogen production catalyzed by positively charged gold nanoparticles. *Int. J. Hydrogen Energy* **2013**, *38*, 5243.
- (15) Yan, Z.; Chinta, S.; Mohamed, A. A.; Fackler, J. P., Jr.; Goodman, D. W. The role of F-centers in catalysis by Au supported on MgO. *J. Am. Chem. Soc.* **2005**, *127*, 1604.
- (16) Brust, M.; Gordillo, G. J. Electrocatalytic hydrogen redox chemistry on gold nanoparticles. *J. Am. Chem. Soc.* **2012**, *134*, 3318.
- (17) Azad, U. P.; Ganesan, V.; Pal, M. Catalytic reduction of organic dyes at gold nanoparticles impregnated silica materials: Influence of functional groups and surfactants. *J. Nanopart. Res.* **2011**, *13*, 3951.
- (18) Cheval, N.; Gindy, N.; Flowkes, C.; Fahmi, A. Polyamide 66 microspheres metallised with in situ synthesized gold nanoparticles for catalytic application. *Nanoscale Res. Lett.* **2012**, *7*, 1.
- (19) Gupta, N.; Singh, H. P.; Sharma, R. K. Metal nanoparticles with high catalytic activity in degradation of methyl orange: An electron relay effect. *J. Mol. Catal. A: Chem.* **2011**, *335*, 248.
- (20) Mallick, K.; Witcomb, M. J.; Scurrall, M. S. Redox catalytic property of gold nanoclusters: Evidence of an electron-relay effect. *Appl. Phys. A: Mater. Sci. Process* **2005**, *80*, 797.
- (21) Carregal-Romero, S.; Pérez-Juste, J.; Hervés, P.; Liz-Marzán, L. M.; Mulvaney, P. Colloidal gold-catalyzed reduction of ferricyanide (III) by borohydride ions: A model system for redox catalysis. *Langmuir* **2009**, *26*, 1271.
- (22) Gao, M.; Lyalin, A.; Taketsugu, T. Role of the support effects on the catalytic activity of gold clusters: A density functional theory study. *Catalysts* **2011**, *1*, 18.
- (23) Han, T. H.; Khan, M. M.; Kalathil, S.; Lee, J.; Cho, M. H. Synthesis of positively charged gold nanoparticles using a stainless steel mesh. *J. Nanosci. Nanotechnol.* **2013**, *13*, 6140.
- (24) Frens, G. Controlled nucleation for the regulation of the particle size in monodisperse gold suspensions. *Nat. Phys. Sci.* **1973**, *241*, 20.
- (25) Logan, B. E.; Murano, C.; Scott, K.; Gray, N. D.; Head, I. M. Electricity generation from cysteine in a microbial fuel cell. *Water Res.* **2005**, *39*, 942.
- (26) Min, B.; Cheng, S.; Logan, B. E. Electricity generation using membrane and salt bridge microbial fuel cells. *Water Res.* **2005**, *39*, 1675.
- (27) Impert, O.; Katafias, A.; Kita, P.; Mills, A.; Pietkiewicz-Graczyk, A.; Wrzeszcz, G. Kinetic and mechanism of fast leuco-Methylene Blue oxidation by copper(II)-halide species in acidic aqueous media. *Dalton Trans.* **2003**, 348.
- (28) Yogi, C.; Kojima, K.; Takai, T.; Wada, N. Photocatalytic degradation of methylene blue by Au-deposited TiO₂ film under UV irradiation. *J. Mater. Sci.* **2009**, *44*, 821.
- (29) Liu, H.; Logan, B. E. Electricity generation using an air-cathode single chamber microbial fuel cell in the presence and absence of a proton exchange membrane. *Environ. Sci. Technol.* **2004**, *38*, 4040.
- (30) Zhang, T.; Oyama, T.; Aoshima, A.; Hidaka, H.; Zhao, J.; Serpone, N. Photooxidative N-demethylation of methylene blue in aqueous TiO₂ dispersions under UV irradiation. *J. Photochem. Photobiol. A: Chem.* **2001**, *140*, 163.
- (31) Mai, F. D.; Chen, C. C.; Chen, J. L.; Liu, S. C. Photodegradation of methyl green using visible irradiation in ZnO suspensions. Determination of the reaction pathway and identification of intermediates by a high-performance liquid chromatography-photo-diode array-electrospray ionization-mass spectrometry method. *J. Chromatogr. A* **2008**, *1189*, 355.
- (32) Yu, H.; Ming, H.; Zhang, H.; Li, H.; Pan, K.; Liu, Y.; Wang, F.; Gong, J.; Kang, Z. Au/ZnO nanocomposites: Facile fabrication and enhanced photocatalytic activity for degradation of benzene. *Mater. Chem. Phys.* **2012**, *137*, 113.
- (33) Kalathil, S.; Lee, J.; Cho, M. H. Gold nanoparticles produced in situ mediate bioelectricity and hydrogen production in a microbial fuel cell by quantized capacitance charging. *ChemSusChem* **2013**, *6*, 246.
- (34) Kalathil, S.; Lee, J.; Cho, M. H. Catalytic role of Au@TiO₂ nanocomposite on enhanced degradation of an azo-dye by electrochemically active biofilms: A quantized charging effect. *J. Nanopart. Res.* **2013**, *15*, 1392.
- (35) Yu, L.; Xi, J.; Li, M. D.; Chan, H. T.; Su, T.; Phillips, D. L.; Chan, W. K. The degradation mechanism of methyl orange under photocatalysis of TiO₂. *Phys. Chem. Chem. Phys.* **2012**, *14*, 3589.
- (36) Khan, M. M.; Kalathil, S.; Han, T. H.; Lee, J.; Cho, M. H. Positively charged gold nanoparticles synthesized by electrochemically active biofilm—A biogenic approach. *J. Nanosci. Nanotechnol.* **2013**, *13*, 6079.